PHYSICAL REVIEW D **79,** 063528 (2009)

Searching for non-Gaussianity in the WMAP data

A. Bernui* and M. J. Rebouças†

Centro Brasileiro de Pesquisas Físicas, Rua Dr. Xavier Sigaud 150, 22290-180 Rio de Janeiro– RJ, Brazil

(Received 20 June 2008; revised manuscript received 16 February 2009; published 30 March 2009)

Some analyses of recent cosmic microwave background (CMB) data have provided hints that there are deviations from Gaussianity in the WMAP CMB temperature fluctuations. Given the far-reaching consequences of such a non-Gaussianity for our understanding of the physics of the early universe, it is important to employ alternative indicators in order to determine whether the reported non-Gaussianity is of cosmological origin, and/or extract further information that may be helpful for identifying its causes. We propose two new non-Gaussianity indicators, based on skewness and kurtosis of large-angle patches of CMB maps, which provide a measure of departure from Gaussianity on large angular scales. A distinctive feature of these indicators is that they provide sky maps of non-Gaussianity of the CMB temperature data, thus allowing a possible additional window into their origins. Using these indicators, we find no significant deviation from Gaussianity in the three and five-year WMAP Internal Linear Combination (ILC) map with *KQ75* mask, while the ILC unmasked map exhibits deviation from Gaussianity, quantifying therefore the WMAP team recommendation to employ the new mask *KQ75* for tests of Gaussianity. We also use our indicators to test for Gaussianity the single frequency foreground unremoved WMAP three and five-year maps, and show that the K and Ka maps exhibit a clear indication of deviation from Gaussianity even with the *KQ75* mask. We show that our findings are robust with respect to the details of the method.

DOI: 10.1103/PhysRevD.79.063528 PACS numbers: 98.80.Es, 98.70.Vc, 98.80.−k

I. INTRODUCTION

Within the standard approach to cosmological modelling the suggestion that the Universe underwent a brief period of rapid acceleration expansion [1] before the epoch of primordial nucleosynthesis has become an essential building block of the standard cosmological model. Besides solving the so-called flatness, horizon, and monopole problems, such a period of cosmological inflation provides a mechanism for the production of the primordial density fluctuations, which seeded the observed cosmic microwave background (CMB) anisotropies and the formation of large-scale structure in the Universe.

There are more than 100 inflationary models (see, e.g., the review articles Refs. [2]), among which the simple ones are based on a slowly rolling single scalar field. An important prediction of a number of these simple models is that they can generate only tiny non-Gaussianity, which should be undetectable in the Wilkinson Microwave Anisotropy Probe (WMAP) CMB data [3]. There are, however, a large class of inflationary models that can generate non-Gaussianity at a level detectable by WMAP [4]. These scenarios comprise models based upon a wide range of mechanisms, including special features of the inflation potential, multiple scalar fields, noncanonical kinetic terms, and nonadiabatic fluctuations (see the review Ref. [5] and references therein). Thus, the detection of non-Gaussianity in CMB data may potentially be useful to discriminate inflationary models and shed light on the physics of the early universe.

In the statistical analyses by using one, three, and five-year [6–9] CMB measurements along with some different statistical tools, the WMAP team has found that the CMB data are consistent with Gaussianity. However, some recent analyses have provided clear hints that there are significant deviations from Gaussianity in the WMAP data. Clearly the study of detectable non-Gaussianities in the WMAP data must take into account that they may have noncosmological origins as, for example, unsubtracted contamination from galactic diffuse foreground emission [10,11] and unconsidered point sources [12]. If they turn out to have a cosmological origin, however, this could have far-reaching consequences on our description of the Universe, particularly on the inflationary picture.

In view of this, a great deal of effort has recently gone into verifying the existence of such non-Gaussianity by employing several different statistical signatures of non-Gaussianity in its various forms (see, e.g., Refs. [13] and related Refs. [14]). Apart from revealing the existence of non-Gaussianity in CMB data, different statistical tools are sensitive to different systematics and may be useful in determining their origins. In addition, different indicators can in principle provide information about the multiple types of non-Gaussianity that may be present in CMB data. It is therefore important to test the data for deviations from Gaussianity by using a range of different statistical tools to identify any non-Gaussian signals on the CMB sky.

In this paper, we propose new large-angle non-Gaussianity indicators, based on skewness and kurtosis of large-angle spherical-shaped patches of CMB maps, which provide a measure of departure from Gaussianity on large angular scales. A distinctive feature of these indicators is that they provide sky maps (directional information) of

*bernui@das.inpe.br
†reboucas@cbpf.br

non-Gaussianity of the CMB temperature fluctuations, thus allowing a possible additional window into their causes. Using these indicators, we find no significant deviation from Gaussianity in the WMAP three and five-year Internal Linear Combination (ILC) *KQ75* masked map, but ILC unmasked map exhibits deviation from Gaussianity. On the other hand, our indicators reveal deviations from Gaussianity of a different degree in the three and five-year single frequency K and Ka *KQ75* masked maps, which is consistent with the fact that even these masked maps are still foreground contaminated at some level.

The structure of the paper is as follows. In Sec. II we introduce our non-Gaussianity indicators. Section III contains the results of applying our statistical indicators to the three-year and five-year WMAP data, and finally in Sec. IV we present the summary of our main results and conclusions.

II. NON-GAUSSIANITY INDICATORS AND MAPS

In this section we construct two statistical indicators that measure the large-angle deviation from Gaussianity of CMB temperature fluctuation patterns.

The main underlying idea in the construction of our non-Gaussianity indicators and the associated maps is that the simplest ways of describing the deviation from symmetry about the CMB mean temperature and a non-Gaussian degree of peakness are by calculating, respectively, the skewness $S = \mu_3/\sigma^3$, and the kurtosis $K = \mu_4/\sigma^4 - 3$ from the data, where μ_3 and μ_4 are the third and fourth central moments of the temperature anisotropies distribution, and σ is the variance. Clearly calculating S and K for the whole celestial sphere would simply yield two dimensionless numbers describing the asymmetry of the data about the CMB average temperature.

However, one can go a step further and obtain directional information about deviation from Gaussianity if instead we take a discrete set of points $\{j = 1, \ldots, N_c\}$ homogeneously distributed on the celestial sphere S^2 as the center of spherical caps of a given aperture γ and calculate S_j and K_j for each cap. The values S_j and K_j can then be viewed as measures of the non-Gaussianity in the direction (θ_j, ϕ_j) of the center of the cap j. Such a study of the individual caps can thus provide information ($2N_c$ numbers) about possible large-angle violation of Gaussianity in the CMB data. A more systematic study can be made by taking the above set of points $\{j\}$ as the center of the pixels for a homogeneous pixelization of S^2 and by choosing caps of large-angle aperture to scan the whole celestial sphere with steps equal to the separation between the centers of adjacent pixels.[1] In this way, we construct two scalar discrete functions S and K defined over the whole celestial sphere that encode measures of non-Gaussianity in CMB data.

This constructive process can be formalized as follows. Let $\Omega_j \equiv \Omega(\theta_j, \phi_j; \gamma) \in S^2$ be a spherical cap, with an aperture of γ degrees, centered at (θ_j, ϕ_j), for $j = 1, \ldots, N_c$. Define the scalar functions S: $\Omega_j \mapsto \mathbb{R}$ and K: $\Omega_j \mapsto \mathbb{R}$, that assign to the jth cap, centered at (θ_j, ϕ_j), two real numbers S_j and K_j given by

$$S_j \equiv \frac{1}{N_p \sigma_j^3} \sum_{i=1}^{N_p} (T_i - \bar{T})^3, \tag{1}$$

$$K_j \equiv \frac{1}{N_p \sigma_j^4} \sum_{i=1}^{N_p} (T_i - \bar{T})^4 - 3, \tag{2}$$

where N_p is the number of pixels in the jth cap, T_i is the temperature at the ith pixel, $\bar{T}$ is the CMB mean temperature, and σ_j is the standard deviation for each j.

We now use the above homogeneously distributed points on S^2 to scan the celestial sphere with evenly distributed spherical caps (of a chosen aperture γ) to calculate S_j and K_j for each cap. Clearly, the numbers S_j and K_j obtained in this way for each cap can then be viewed as a measure of non-Gaussianity in the direction of the center of that cap (θ_j, ϕ_j). Patching together the S_j and K_j values for each cap, we obtain the indicators that are discrete functions $S = S(\theta, \phi)$ and $K = K(\theta, \phi)$ defined over the celestial sphere, which measure the deviation from Gaussianity as a function of direction (θ, ϕ). In this way, $S = S(\theta, \phi)$ and $K = K(\theta, \phi)$ give a scalar directional measure of non-Gaussianity over the celestial sphere.

Now, since $S = S(\theta, \phi)$ and $K = K(\theta, \phi)$ are discrete scalar functions defined on S^2 they can also be viewed as maps of non-Gaussianity, and we can expand each of these functions in their spherical harmonics and calculate their angular power spectrum. Thus, for the skewness function $S = S(\theta, \phi)$, for example, one has

$$S(\theta, \phi) = \sum_{\ell=0}^{\infty} \sum_{m=-\ell}^{\ell} b_{\ell m} Y_{\ell m}(\theta, \phi) \tag{3}$$

and can calculate the corresponding angular power spectrum

$$S_\ell = \frac{1}{2\ell + 1} \sum_m |b_{\ell m}|^2 \tag{4}$$

in order to further quantify the angular scale information regarding the deviation from Gaussianity of CMB data. Clearly, one can similarly expand the kurtosis function $K = K(\theta, \phi)$ and calculate its angular power spectrum K_ℓ. It then follows that, if a large-scale non-Gaussianity is present in the original temperature distribution, it should significantly affect the S and K maps on the corresponding angular scales.

[1] Note that here this pixelization is only a practical way of choosing the centers of the caps homogeneously distributed on S^2. It is not related to the pixelization of the CMB maps.

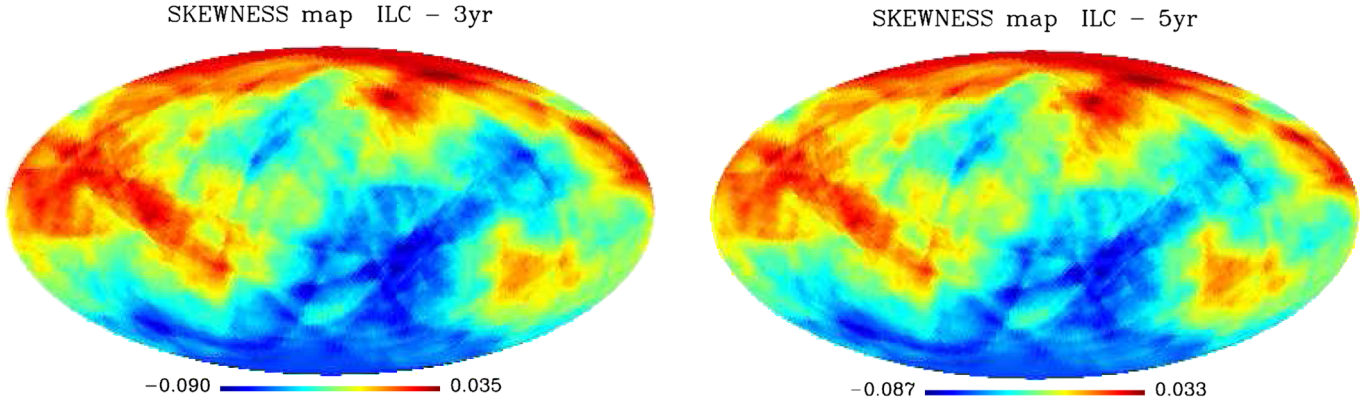

FIG. 1 (color online). Skewness indicator maps from the WMAP three (left panel) and five-year (right panel) ILC maps with mask *KQ75*.

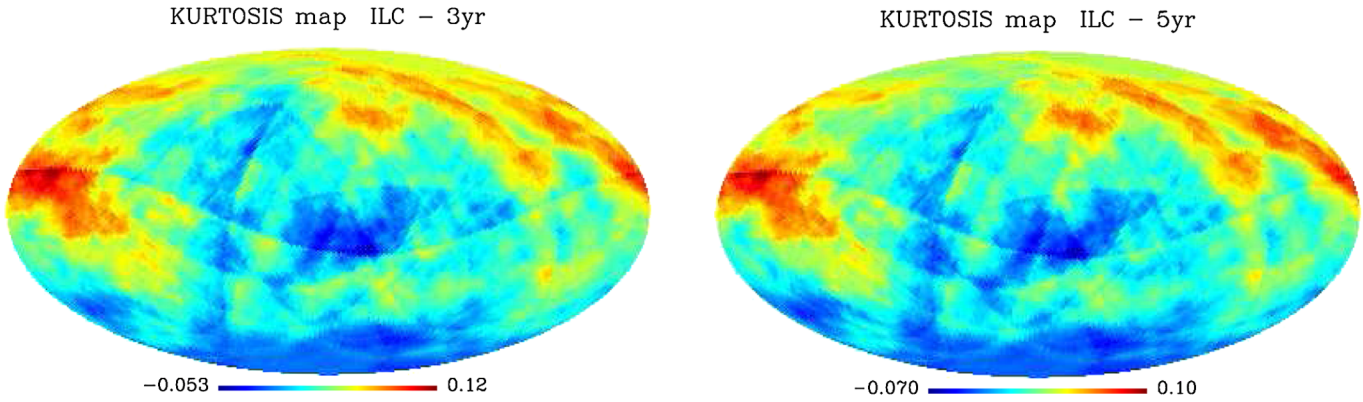

FIG. 2 (color online). Kurtosis indicator maps from the WMAP three (left panel) and five-year (right panel) ILC maps with mask *KQ75*.

In the next section we shall apply the indicators $S = S(\theta, \phi)$ and $K = K(\theta, \phi)$ to both WMAP three and five-year data.

III. NON-GAUSSIANITY INDICATORS AND WMAP DATA

The WMAP team has produced high angular resolution maps of the CMB temperature fluctuations in five frequency bands: K-band (22.8 GHz), Ka-band (33.0 GHz), Q-band (40.7 GHz), V-band (60.8 GHz), and W-band (93.5 GHz). Following the WMAP team recommendation for tests of Gaussianity [8,15], we used the ILC maps of both the three-year and the five-year CMB data [16] along with the new mask *KQ75*, which is slightly more conservative than the *Kp0*, i.e., *KQ75* sky cuts is 28.4% while *Kp0* cuts is 24.5%. We also test for non-Gaussianity the ILC full-sky five-year map along with the five frequency foreground uncleaned five-year maps with and without the *KQ75* mask. In all cases we chose the HEALPix parameter $N_{\rm side} = 256$ [17], which corresponds to a partition of the celestial sphere into 786 432 pixels.

In our calculations of skewness and kurtosis indicator maps (hereafter referred to as *S*-map and *K*-map) from each CMB map we have scanned the celestial sphere with spherical caps of aperture $\gamma = 90°$, centered at $N_{\rm c} = 768$, 3072, and 12 288 points homogeneously generated on the sphere by using HEALPix. However, to avoid repetition we only present a detailed analysis for $N_{\rm c} = 12\,288$ in the following.

Figures 1 and 2 show, respectively, the Mollweide projection of the *S* map and *K* map in galactic coordinates obtained from the ILC WMAP three (left panels) and five-year (right panels) maps with the *KQ75* mask. They clearly show that the $S(\theta, \phi)$ and $K(\theta, \phi)$ distributions of hot and cold spots (higher and lower values) for the indicators are not evenly distributed in the celestial sphere, suggesting at first sight non-Gaussianity of the ILC masked data. The comparison between the two *S* maps (Fig. 1) and the two *K* maps (Fig. 2) shows a great number of similarities for each pair of maps of the indicators, which is a very first indication of the robustness of our results with respect to the three and five-year WMAP data.[2] Figures 1 and 2 are also

[2]It is interesting to note the presence of great circles of unknown origin near the galactic plane in the *K* maps and in a less accentuated way in the *S* maps.

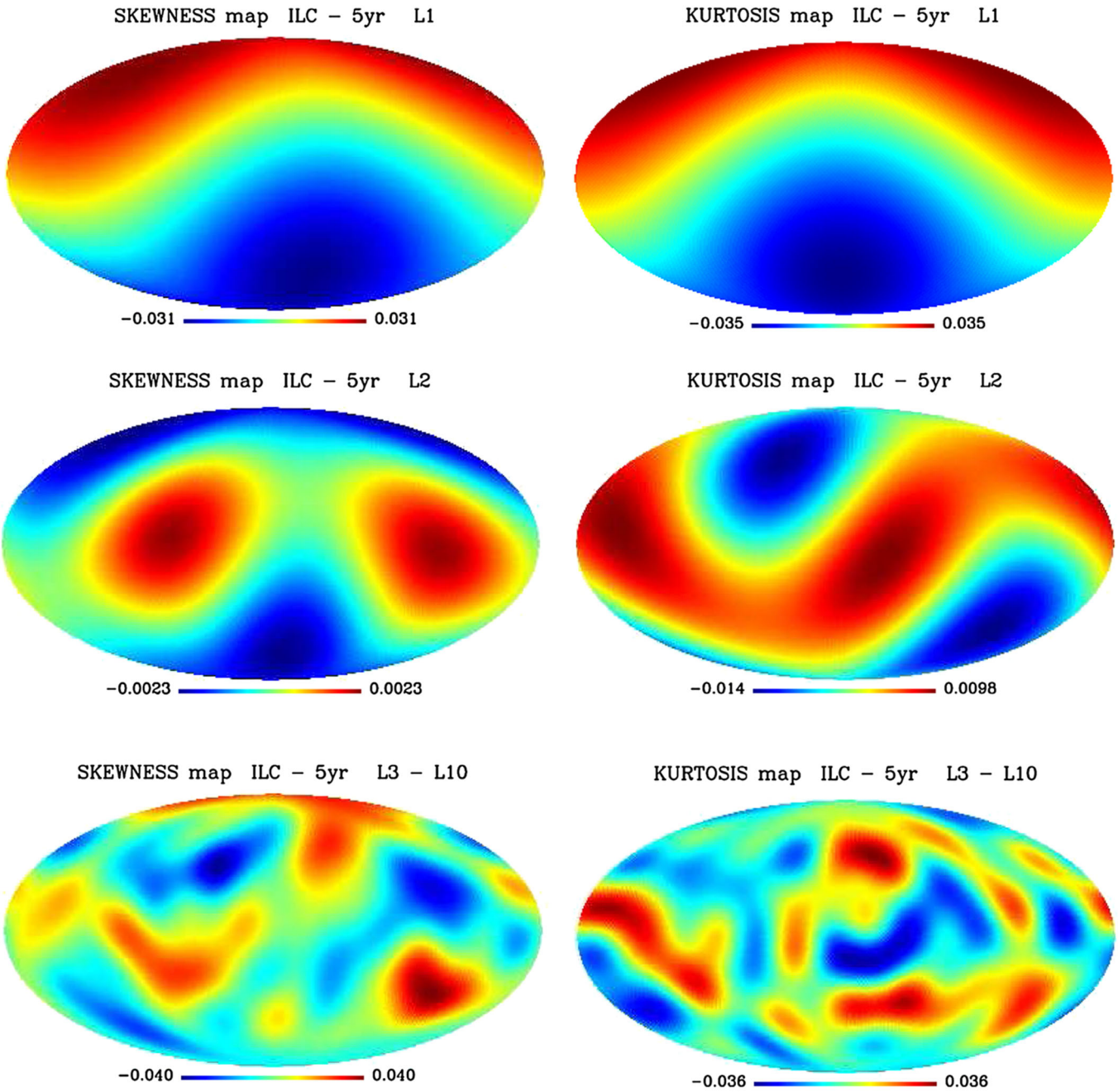

FIG. 3 (color online). Depicted the dipole, quadrupole, and the remaining low ℓ components for the skewness (left panels) and kurtosis (right panels) maps obtained from the five-year WMAP ILC with mask *KQ75*.

suggestive of large-scale components in the maps of both indicators.

To provide some additional qualitative information about the anisotropic distribution of our non-Gaussianity indicators, we depict in Fig. 3 the dipole and the quadrupole as well as the full S and K maps with these two components and the monopole removed. The left panels display these components for the skewness indicator $S(\theta, \phi)$, while the right panels show the same components for the kurtosis indicator $K(\theta, \phi)$. These multipole maps were calculated from the WMAP five-year ILC masked data, but corresponding maps for three-year WMAP data are largely similar to the depicted maps and were not included to avoid repetition.

It is known that the frequency K-band, Ka-band, Q-band, V-band, and W-band foreground uncleaned maps have different contaminants. These features may appear in these maps in the form of non-Gaussianity even when the *KQ75* mask is utilized. Thus, in order to suitably test the S and K indicators for non-Gaussianity one should

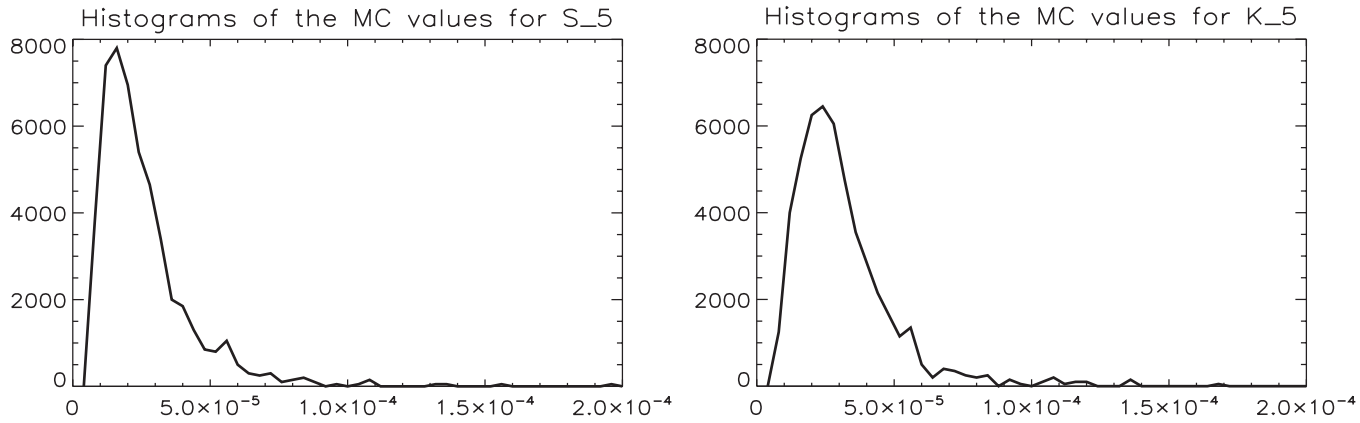

FIG. 4. Histograms show the distribution of the values for the multipoles S_5 and K_5 calculated from the MC (*scrambled*) ILC maps. This figure illustrates the non-Gaussianity of a typical distribution for a given fixed ℓ.

calculate their maps and angular power spectra not only for the foreground-reduced ILC masked and unmasked maps, but also for these single frequency maps with and without *KQ75* mask. This also allows a comparative analysis of the outcomes. To this end, we have also calculated the S maps and K maps for each of these five frequency maps with and without *KQ75* mask, for caps with aperture $\gamma = 90°$, centered at $N_c = 12\,288$ points homogeneously generated on the sphere by using HEALPix. However, to avoid repetition of figures which give only qualitative information, in the following we shall concentrate on their angular power spectra, which provide quantitative information.

We calculated the angular power spectrum of the S and K maps generated from the three and five-year data of ILC and the foreground unreduced K, Ka, Q, V, and W maps with and without *KQ75* mask. These power spectra allow to estimate the statistical significance of S_ℓ and K_ℓ by comparing them with the mean angular power spectrum of the S and K maps obtained from 1000 Monte Carlo-generated (MC) statistically Gaussian CMB maps.[3] To make easier this comparison, instead of using the angular power spectra S_ℓ and K_ℓ themselves, we employed the *differential* power spectra $|S_\ell - \bar{S}_\ell|$ and $|K_\ell - \bar{K}_\ell|$. Throughout the paper the mean quantities are denoted by an overline.

To describe with some details our calculations we focus on the skewness indicator S, since a similar procedure holds for the kurtosis indicator K. Starting from a given CMB seed map (ILC or any frequency band map) we generated 1000 MC Gaussian (*scrambled*) CMB maps, which are then used to generate 1000 skewness S maps, from which we calculate 1000 power spectra: $S_\ell^{\mathbf{i}}$ with enumeration index $\mathbf{i} = 1, \cdots, 1000$. In this way, for each fixed multipole component $S^{\mathbf{i}}_{\ell=\text{fixed}}$ we have 1000 values from which we calculate the mean value $\bar{S}_\ell = (1/1000) \times \sum_{\mathbf{i}=1}^{1000} S_\ell^{\mathbf{i}}$. From this MC process we have at the end ten mean values $\bar{S}_\ell$ each of which are then used to compare with the corresponding power spectrum component S_ℓ of the skewness map obtained from an *unscrambled* seed temperature WMAP map, in order to evaluate the statistical significance of each multipole component. Thus, for example, to study the statistical significance of the dipole moment of the skewness-ILC map S_1^{ILC} we calculate $|S_1^{\text{ILC}} - \bar{S}_1|$, where the mean dipole value $\bar{S}_1$ is calculated from the $\mathbf{i} = 1, \cdots, 1000$ power spectra of the Gaussian (*scrambled*) maps.

The panels of Fig. 4 display the histograms which show the distribution of the values for S_5 and K_5 calculated from the *scrambled* ILC maps. This figure makes clear that a typical distribution of MC values for a given fixed ℓ is highly non-Gaussian.

Figure 5 shows the differential power spectra calculated from *full-sky* CMB five-year maps, i.e., it displays the absolute value of the deviations from the mean angular power spectrum of the skewness S_ℓ (left panel) and kurtosis K_ℓ (right panel) indicators for $\ell = 1, \cdots, 10$, which is a range of multipole values useful to investigate the large-scale angular characteristics of the S and K maps. This figure makes apparent the strong deviation from Gaussianity of the unmasked frequency maps. This is expected from the very outset since these full-sky band maps are highly contaminated. Figure 5 also shows a significant deviation from Gaussianity in five-year ILC unmasked data, i.e. the deviations $|S_\ell - \bar{S}_\ell|$ and $|K_\ell - \bar{K}_\ell|$ for the five-year ILC unmasked data are not within 95% of the MC value. Actually the values of S_ℓ and K_ℓ obtained from the data are far beyond ($\gg 95\%$ off) the mean MC values (see Fig. 5). These results quantify and make clear the suitability of the WMAP team recommendation to employ the new mask *KQ75* for tests of Gaussianity. These spectra maps were calculated from

[3]We note that each MC map is a stochastic realization of the WMAP best-fitting angular power spectrum of the ΛCDM model, obtained by randomizing the multipole temperature components $a_{\ell m}$ within the cosmic variance limits [8,18].

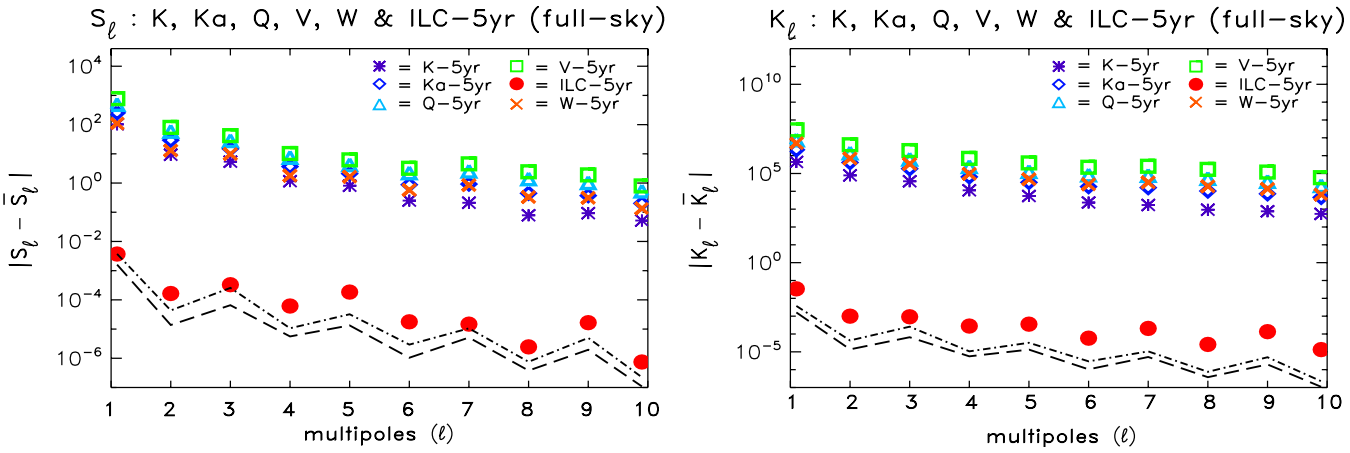

FIG. 5 (color online). Differential power spectrum of skewness $|S_\ell - \bar{S}_\ell|$ and $|K_\ell - \bar{K}_\ell|$ (left) and kurtosis (right) indicators calculated from the and five-year (right panels) WMAP CMB maps with no mask. The 68% and 95% confidence levels are indicated, respectively, by the dashed and dash-dotted lines.

the WMAP five-year data, but the corresponding spectra for three-year data are very similar to the depicted spectra. We stress that for the frequency maps we have used the foreground uncleaned maps as the temperature fluctuations seed maps.

Figure 6 shows similar differential power spectra but now calculated from the CMB three and five-year maps with *KQ75* mask. Tables I and II complement Fig. 6 by collecting together the percentage of the deviations $|S^{\mathbf{i}}_\ell - \bar{S}_\ell|$ (calculated from 1000 *scrambled* MC simulated maps) which are smaller than $|S_\ell - \bar{S}_\ell|$ obtained from the data, i.e. from the five-year ILC, K, Ka, Q, V, and W masked maps. Thus, for example, according to Table I for the K-band 99.6% of multipoles $S^{\mathbf{i}}_3$ obtained from the MC maps are closer to the mean $\bar{S}_3$ than the value S_3 calculated from the K map (three and five-year data). This indicates how unlikely (only 0.4%) the occurrence of the value obtained from the data for the multipole S_3 in the set of MC simulated maps for this band is, giving therefore a clear indication of deviation from Gaussianity for the K masked maps to the extent that this is not within ~95% of MC values.

Regarding the angular power spectrum of the skewness and kurtosis maps calculated from the ILC maps with *KQ75* mask, it is clear from Fig. 6 and Tables I and II that the low ℓ multipole ($\ell = 1, \cdots, 10$) values—indicative of large-angle deviation from Gaussianity—are not statistically significant, i.e. they are within ~95% of the MC values. In other words, the occurrence of these ILC multipole values is very likely ($\geq$ 5%) in the set of MC values.[4] It is interesting to note that a comparison between Figs. 5 and 6 makes apparent the important role of the mask in the test for Gaussianity carried out. Furthermore, Fig. 6 and Tables I and II also show that this analysis is robust with respect to the three and five-year ILC maps.

As regards the angular power spectra of S and K calculated from the K-band map with *KQ75* mask, it is clear from Fig. 6 and Tables I and II that both the skewness and kurtosis spectra reveal deviations from the mean power spectrum values, greater than 95%, for $\ell = 2, 3, 5, 6, 7, 8, 10$. This indication of deviation from Gaussianity comes chiefly from the fact that even with the *KQ75* mask the K-band map is still foreground contaminated as illustrated in the first row [panels (a) and (b)] of Fig. 7.

Figure 7 [second row, panels (c) and (d)] suggests a residual foreground contamination in the Ka-band map with *KQ75* mask. This remnant contamination from galactic foreground emission is detected by the kurtosis indicator K, whose power spectrum shows an excess of power relative to the mean for $\ell = 1, 7, 9$ components [see the second row of panels in Fig. 6 and Table II].

Regarding the angular power spectra of the S and K indicators for the remaining three and five-year frequency maps (Q, V, W) with *KQ75* mask the panels of Fig. 6 along with Tables I and II show that the occurrence of the power spectrum low ℓ values calculated from these frequency maps are very likely ($>$ 5%) in the set of MC values, i.e. the Q, V, and W multipole values are well within $\simeq$ 95% of MC values. This makes it clear that for these frequency maps the *KQ75* mask reduces considerably the contamination to a level which makes the power spectra of this masked map compatible with Gaussianity.

These results of our statistical analyses indicate that the current CMB temperature fluctuations of the ILC foreground-reduced three and five-year *KQ75* masked maps are consistent with Gaussianity in that the occurrence of these ILC multipole values is very likely ($\geq$ 5%) in the set of MC values, i.e. the ILC multipole values of the S and K are within $\simeq$ 95% of the MC values of the *scrambled*

[4]We note that the values of S_6 (five-year) and K_5 (five-year) are slightly smaller than 5%.

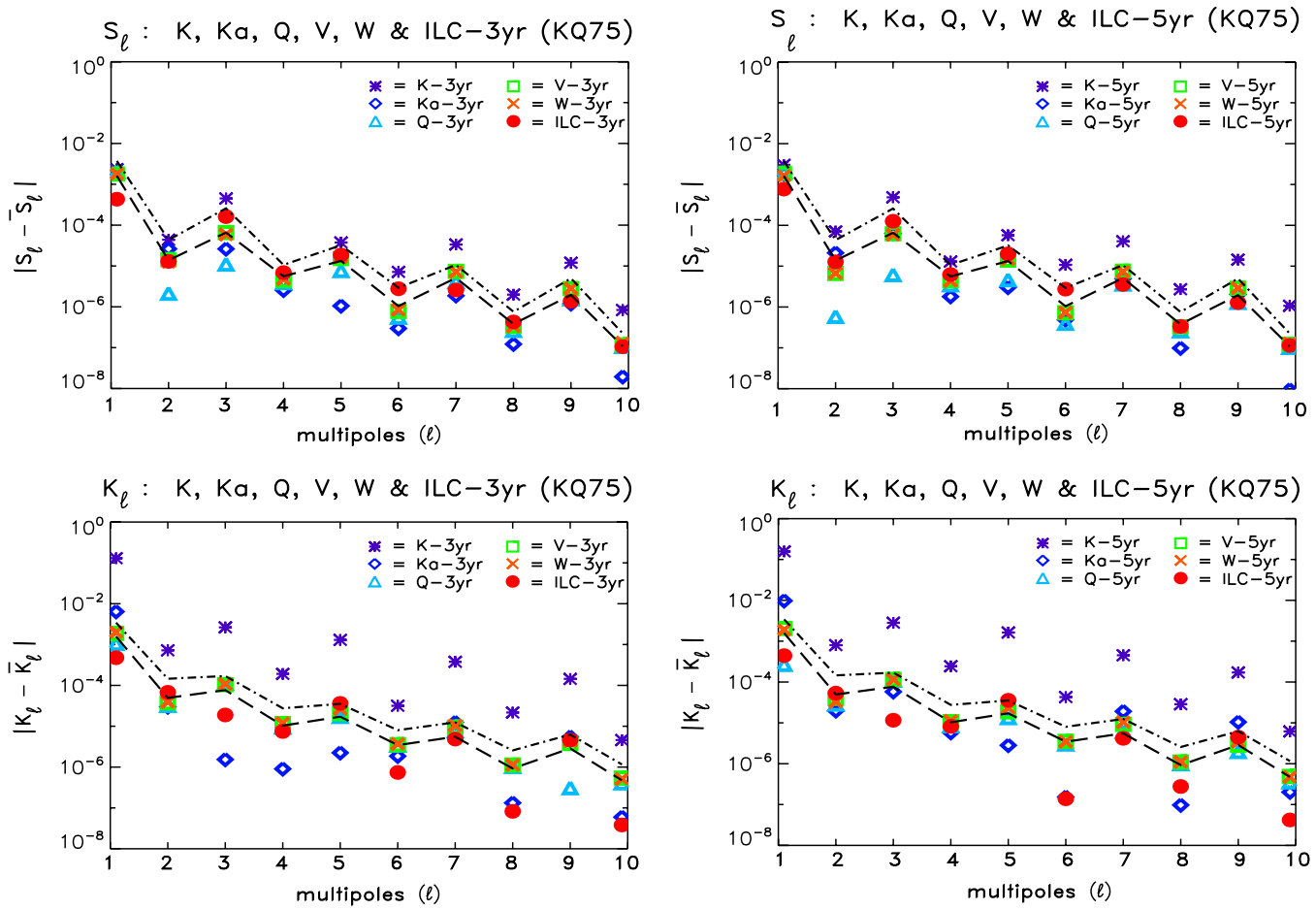

FIG. 6 (color online). Differential power spectrum of skewness (first row) and kurtosis (second row) indicators calculated from the three (left panels) and five-year (right panels) WMAP CMB maps with mask *KQ75*. The 68% and 95% confidence levels are indicated, respectively, by the dashed and dot-dashed lines. See the text for more details.

(Gaussian) maps. This result agrees with the WMAP team and other analyses made by using different statistical tools [6–9]. On the other hand, our analyses detect a deviation from Gaussianity in the three and five-year frequency *KQ75* masked K and Ka maps which is consistent with the fact that even these masked maps are foreground contaminated at some level (see Fig. 7). As for the Q, V, and W frequency unremoved foreground maps, our analyses indicate that although considerably contaminated in their full-sky form (as captured in Fig. 5), *KQ75* mask cuts the

TABLE I. Percentage of the deviations $|S^{\mathrm{i}}_\ell - \bar{S}_\ell|$ (for $\ell = 1, \cdots, 10$ and calculated from 1000 *scrambled* MC simulated maps), which are smaller than $|S_\ell - \bar{S}_\ell|$ obtained from the data: S maps generated from the three (left entries of each column) and five-year (right accesses for each column) CMB maps in the frequencies K (22.8 GHz), Ka (33.0 GHz), Q (40.7 GHz), V (60.8 GHz), and W (93.5 GHz), along with the ILC three and five-year maps.

ℓ	K	Ka	Q	V	W	ILC
1	90.6–93.2	83.7–76.4	88.5–88.7	74.5–80.6	76.0–66.4	14.8–26.3
2	95.9–97.7	92.3–90.1	6.5–1.3	70.5–22.8	57.2–23.2	59.0–57.9
3	99.6–99.6	24.1–63.6	10.0–5.7	66.1–61.5	57.7–57.5	96.3–94.3
4	71.0–94.4	23.7–16.0	39.0–34.3	47.0–46.6	52.3–45.6	90.0–83.7
5	96.4–98.4	6.4–16.1	38.8–21.9	74.6–70.1	80.8–72.4	86.0–88.7
6	99.5–99.7	16.7–30.1	34.2–23.6	45.8–42.5	51.5–43.3	96.2–96.0
7	99.7–99.7	24.4–64.1	53.0–46.7	88.7–89.3	87.5–88.6	33.4–45.9
8	99.5–99.7	19.0–16.0	43.8–43.4	59.4–57.7	58.8–57.8	83.7–59.4
9	99.6–99.7	41.6–70.7	53.4–45.4	87.1–87.9	87.2–88.2	47.0–45.0
10	99.8–99.8	10.1–4.1	67.5–63.4	75.4–77.6	82.9–81.9	66.0–72.3

TABLE II. Percentage of the deviations $|K_\ell^{\mathrm{i}} - \bar{K}_\ell|$ (calculated from 1000 *scrambled* MC random maps for $\ell = 1, \cdots, 10$), which are smaller than $|K_\ell - \bar{K}_\ell|$ obtained from the data: K maps generated from the three (left entries of each column) and five-year (right entries for each column) CMB seed maps in the channels K (22.8 GHz), Ka (33.0 GHz), Q (40.7 GHz), V (60.8 GHz), and W (93.5 GHz), along with the ILC three and five-year maps.

ℓ	K	Ka	Q	V	W	ILC
1	99.9–99.9	98.7–99.3	44.5–11.7	82.0–87.8	86.4–82.6	19.4–18.9
2	99.9–99.9	27.1–14.1	29.8–25.2	38.4–42.1	41.6–30.3	74.9–76.4
3	99.9–99.9	1.7–51.5	90.1–89.5	86.9–90.9	88.7–90.8	16.0–10.9
4	99.8–99.8	3.0–24.8	55.4–45.6	84.8–72.3	89.1–79.6	37.2–42.9
5	99.9–99.9	7.9–10.5	69.4–54.3	80.1–74.1	93.2–87.6	94.7–95.3
6	99.8–99.8	21.0–2.2	66.1–49.2	73.0–71.7	80.1–67.4	8.3–1.9
7	99.9–99.9	95.1–97.9	86.5–74.9	92.5–91.8	93.7–93.7	60.3–53.1
8	99.8–99.8	7.2–4.8	82.8–76.9	91.8–90.0	93.2–90.7	4.3–13.4
9	99.9–99.9	94.8–97.9	5.9–47.4	85.6–68.8	92.3–81.0	93.5–95.0
10	99.8–99.8	3.2–17.1	48.7–37.1	89.2–73.3	80.4–67.1	2.2–2.3

galactic regions so as to bring their S and K power spectra to a level consistent with Gaussianity (the multipole values are within ~95% of MC values).

Finally, to have an overall assessment of the power spectra of the S and K maps calculated from each CMB seed map we have performed a χ^2 test to find out the goodness of fit for S_ℓ and K_ℓ multipole values as compared to the expected multipole values from the Gaussian MC maps. In this way we can obtain one number that collectively quantifies the extent to which a given *KQ75* masked map is consistent with Gaussianity. For the power spectra S_ℓ we found that the ratio χ^2/dof (dof stands for degrees of freedom) from the K, Ka, Q, V, W, and ILC maps are given, respectively, by 21.5, 4.9, 6.0, 5.2, 3.9, and 1.2, while for

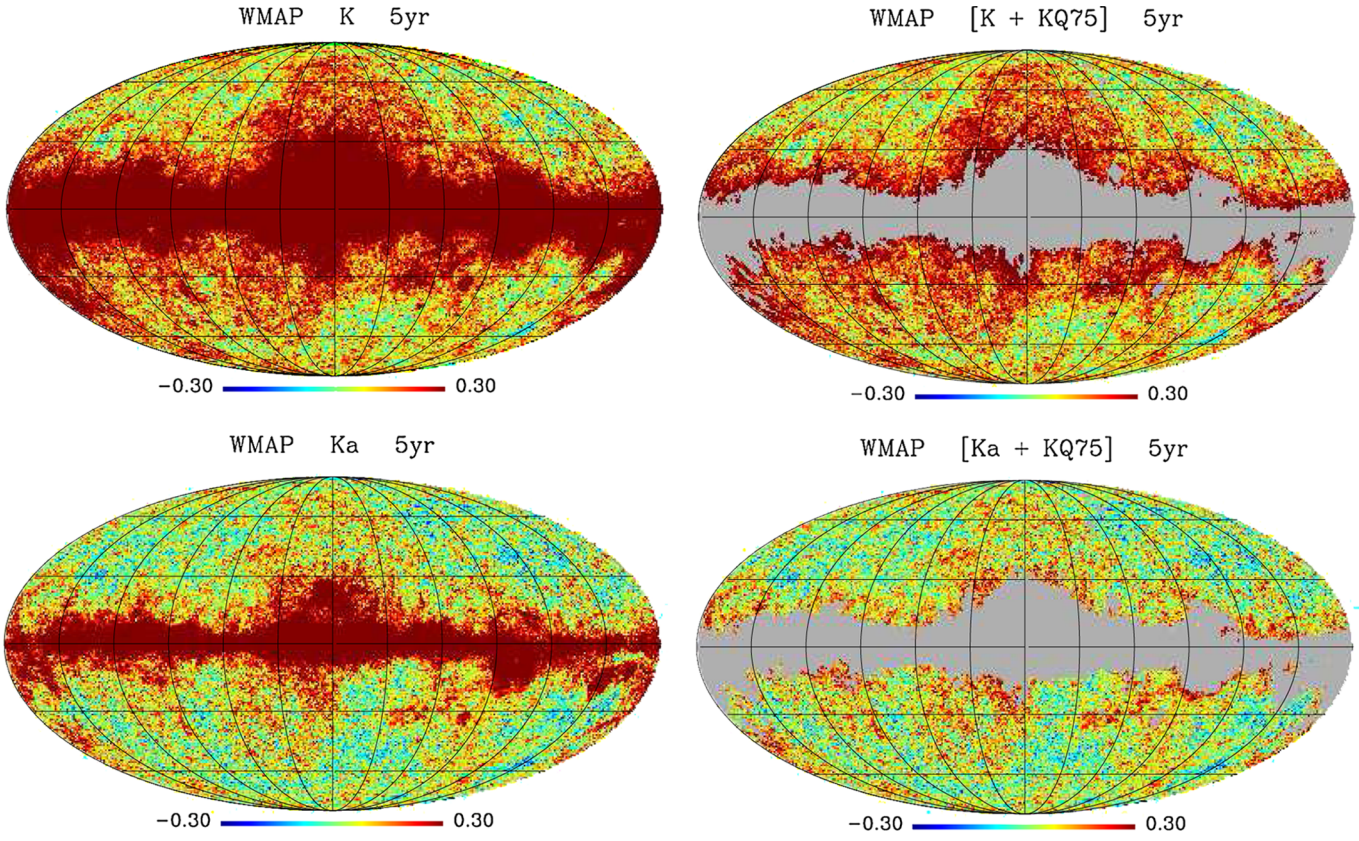

FIG. 7 (color online). CMB temperature fluctuations five-year maps in the frequencies K (22.8 GHz) and Ka (33.0 GHz) without (left panel) and with the mask *KQ75*. These figures illustrated that even these masked maps are still foreground contaminated at some level. These signs of deviation from Gaussianity in the *KQ75* masked maps are captured by our indicators S (K *KQ75* masked map) and K (K and Ka *KQ75* masked maps).

the kurtosis power spectra K_ℓ of these maps the values of χ^2/dof are, respectively, 35 652, 135, 0.5, 6.4, 5.6, and 0.4. Clearly the greater these values are the smaller the χ^2 probability is, i.e., the probability that the multipole values S_ℓ and K_ℓ (from each CMB maps) and the expected MC multipole values agree. A cutoff value of $\chi^2/\mathrm{dof} \simeq 7$ to reject the hypothesis that the multipole values S_ℓ and K_ℓ are a good approximation to the expected multipole values of MC Gaussian realizations, is therefore enough to ensure that Q, V, W, and ILC *KQ75* masked are consistent with Gaussianity, while the K and Ka (*KQ75* masked) maps are not.

The calculations of our non-Gaussianity indicators require not only the choice of a CMB map as input, but also the specification of some quantities whose choice could in principle affect the outcome of our results. To test the robustness of our scheme, hence of our results, we studied the effects of changing various parameters employed in the calculation of our indicators. We found that the S and K angular power spectra do not change appreciably as we change the WMAP ILC three-year and five-year maps; the resolution of CMB temperature maps used (786 432 or 3 145 728 pixels); and the number of point centers of the caps with values 768, 3072, and 12 288. The deviations from the mean power spectrum for three-year and five-year frequency band maps are also robust (see Tables I and II).

Concerning the robustness of the above analyses some additional words of clarification are in order here. First, we note that the calculations of the S maps and K maps by scanning the CMB maps sometimes include caps whose center is within or close to the *KQ75* masked region. In these cases, the calculations of these indicators are made with a smaller number of pixels, which clearly introduce additional statistical noise as compared to the cases whose caps centers are far away from the mask. In order to minimize this effect we have scanned the CMB sky with spherical caps of aperture $\gamma = 90°$.[5]

Second, we have checked the sensitivity of our results regarding ILC maps with respect to the angular resolution of CMB maps, the number N_c of point centers of the caps used to scan the CMB sky, and the aperture γ of the caps by carrying out correlation analyses between the resultant S and K maps calculated for CMB maps with 3 145 728, and 786 432 pixels along with $N_c = 768$, 3072, and 12 288. We found that for $\gamma = 90°$ the resulting S and K maps are strongly correlated according to Pearson's correlation coefficient. Thus, for example, for the S maps calculated from the two CMB pixelizations the Pearson's correlation coefficients are equal to 99.995%, 99.995%, and 99.996% for $N_c = 768$, 3072, and 12 288, respectively, while for the K maps this coefficient is 99.996% for the three values of N_c. However, for caps with aperture $\gamma = 70°$, for example, the Pearson's correlation coefficients for S and K maps (calculated for CMB maps with these two pixelizations and the same values of N_c) fall below 50%, making clear that caps of aperture $\gamma = 90°$ are the most suitable spherical caps to deal with the statistical noise in our scheme.

IV. FINAL REMARKS AND CONCLUSIONS

We have proposed two new indicators for measuring large-angle directional deviations from Gaussianity in the CMB data and have used them to search for the large-angle (low ℓ) deviation from Gaussianity in the three and five-year foreground-reduced ILC and the five single frequency (K, Ka, Q, V, W) *KQ75* masked maps. Our directional indicators enable us to construct skewness S and kurtosis K maps (as, e.g., Figs. 1 and 2), making it possible to examine the presence and significance of possible large-angle non-Gaussianity in the WMAP CMB temperature fluctuations maps with and without *KQ75* mask.

To obtain a more quantitative measure of non-Gaussianity we have studied the low ℓ angular power spectrum of the S and K maps generated from the (three and five-year) WMAP ILC and frequency (unremoved foreground) maps with and without *KQ75* mask. For the full-sky ILC maps we found deviation from Gaussianity for the low ℓ, while for the ILC masked maps we found that the low ℓ ($\ell = 1, \cdots, 10$) components are not significantly different from corresponding components of the expected power spectrum calculated from S and K maps obtained from 1000 Monte Carlo CMB maps generated by considering the Gaussian random hypothesis based on the concordance model [8]. Actually, we have found that the values of the multipoles S_ℓ and K_ℓ (for $\ell = 1, \cdots, 10$) are not statistically significant, i.e. they are within the 95% values of S_ℓ's and K_ℓ's of the MC randomly scrambled maps (Fig. 6 and Tables I and II). As regards the frequency maps, we found clear indication of deviation from Gaussianity in the three and five-year frequency *KQ75* masked maps: K and Ka, which is expected and consistent with the fact that even these masked maps present some level of foreground contamination away from the masked region (see Fig. 7). The deviation for the Q, V, and W masked maps are within the 95% expected values from MC randomly simulated maps.

[5]Note that even in the case of 90° caps the sky regions whose centers are within or close to the galaxy have smaller sky fraction than those centered far away from the mask. This could lead to bias in our non-Gaussianity estimators. A possible way to circumvent this problem is by dividing S_j and K_j by the corresponding standard deviation $(\overline{S_j^2} - \overline{S_j}^2)^{1/2}$ or $(\overline{K_j^2} - \overline{K_j}^2)^{1/2}$, obtained by using MC CMB seed maps. We have calculated the maps and power spectra for these normalized indicators for 1000 MC maps. It turns out that for $\gamma = 90°$ caps, the power spectra of normalized and unnormalized indicators, calculated for the WMAP ILC five-year map, essentially coincide. For caps of smaller aperture as, e.g., $\gamma = 60°$, although the normalization gives rise to smaller powers for S_ℓ and K_ℓ, the loss of powers for each ℓ is not enough to make the $\gamma = 60°$ results close to the clearly statistically less noisy $\gamma = 90°$ power spectrum estimates.

To have an overall quantitative assessment of the power spectra S_ℓ and K_ℓ calculated from K, Ka, Q, V, W, and ILC maps we have performed a χ^2 test to determine the goodness of fit for low ℓ multipole values as compared to the expected multipole values from the Gaussian MC maps. In this way we have obtained numbers that collectively quantify the extent to which these *KQ75* masked maps are consistent with Gaussianity.

The results of our statistical analyses indicate that the current CMB temperature fluctuations ILC three and five-year masked data are consistent with Gaussianity, in agreement with the WMAP team and other analyses made by using different statistical tools [6–8]. We have demonstrated that the results of our analyses are robust by showing that the S map and K map do not significantly change with different choices of variables involved in our scheme, so long as the statistical noise is kept under control.

The effects of different foreground-reduced algorithms as detected by our non-Gaussianity indicators for other WMAP three and five-year maps [19–21] are under careful investigation and signs of non-Gaussianity seem to be present in the maps, which may have a noncosmological origin as, for example, residual foregrounds, artifacts of the cleaning algorithm, or simply a statistical fluke.

Finally, we emphasize that the robustness of our scheme with respect to all considered parameters along with the detection on non-Gaussianity in the single frequency (foreground unremoved) maps seem to indicate that our indicators are well suited to reliably map deviation from Gaussianity at large angular scales in the CMB data, besides being complementary to the other approaches in the literature.

ACKNOWLEDGMENTS

This work is supported by Conselho Nacional de Desenvolvimento Científico e Tecnológico (CNPq)—Brasil, under Grant No. 472436/2007-4. M. J. R. and A. B. thank CNPq and PCI-CBPF/CNPq for the grants under which this work was carried out. We thank an anonymous referee for her/his constructive and careful reports that has led to the substantial improvement of the article. We are also grateful to A. F. F. Teixeira for reading the manuscript and indicating the omissions and misprints. We acknowledge use of the Legacy Archive for Microwave Background Data Analysis (LAMBDA). Some of the results in this paper were derived using the HEALPix package [17].

[1] A. A. Starobinsky, JETP Lett. **30**, 682 (1979) [Pis'ma Zh. Eksp. Teor. Fiz. **30**, 719 (1979)]; Phys. Lett. B **117**, 175 (1982); D. Kazanas, Astrophys. J. **241**, L59 (1980); A. H. Guth, Phys. Rev. D **23**, 347 (1981); K. Sato, Mon. Not. R. Astron. Soc. **195**, 467 (1981); A. D. Linde, Phys. Lett. B **108**, 389 (1982); A. Albrecht and P. J. Steinhardt, Phys. Rev. Lett. **48**, 1220 (1982).

[2] B. A. Bassett, S. Tsujikawa, and D. Wands, Rev. Mod. Phys. **78**, 537 (2006); A. Linde, Lect. Notes Phys. **738**, 1 (2008).

[3] V. Acquaviva, N. Bartolo, S. Matarrese, and A. Riotto, Nucl. Phys. **B667**, 119 (2003); J. Maldacena, J. High Energy Phys. 05 (2003) 013; M. Liguori, F. K. Hansen, E. Komatsu, S. Matarrese, and A. Riotto, Phys. Rev. D **73**, 043505 (2006).

[4] N. Arkani-Hamed, P. Creminelli, S. Mukohyama, and M. Zaldarriaga, J. Cosmol. Astropart. Phys. 04 (2004) 001; N. Bartolo, S. Matarrese, and A. Riotto, Phys. Rev. D **69**, 043503 (2004); D. H. Lyth and Y. Rodriguez, Phys. Rev. D **71**, 123508 (2005); G. I. Rigopoulos, E. P. S. Shellard, and B. J. W. van Tent, Phys. Rev. D **73**, 083522 (2006); L. E. Allen, S. Gupta, and D. Wands, J. Cosmol. Astropart. Phys. 01 (2006) 006; X. Chen, Phys. Rev. D **72**, 123518 (2005); N. Barnaby and J. M. Cline, Phys. Rev. D **73**, 106012 (2006); **75**, 086004 (2007); J. Cosmol. Astropart. Phys. 07 (2007) 017; M. Sasaki, J. Valiviita, and D. Wands, Phys. Rev. D **74**, 103003 (2006); X. Chen, M.-X. Huang, S. Kachru, and G. Shiu, J. Cosmol. Astropart. Phys. 01 (2007) 002; X. Chen, R. Easther, and E. A. Lim, J. Cosmol. Astropart. Phys. 06 (2007) 023; T. Battefeld and R. Easther, J. Cosmol. Astropart. Phys. 03 (2007) 020; H. Assadullahi, J. Valiviita, and D. Wands, Phys. Rev. D **76**, 103003 (2007); D. Battefeld and T. Battefeld, J. Cosmol. Astropart. Phys. 05 (2007) 012; R. Bean, S. E. Shandera, S. H. Henry Tye, and J. Xu, J. Cosmol. Astropart. Phys. 05 (2007) 004; M. Kawasaki, K. Nakayama, T. Sekiguchi, T. Suyama, and F. Takahashi, J. Cosmol. Astropart. Phys. 11 (2008) 019; 01 (2009) 042; M. Kawasaki, K. Nakayama, and F. Takahashi, J. Cosmol. Astropart. Phys. 01 (2009) 026.

[5] N. Bartolo, E. Komatsu, S. Matarrese, and A. Riotto, Phys. Rep. **402**, 103 (2004).

[6] E. Komatsu *et al.*, Astrophys. J. Suppl. Ser. **148**, 119 (2003).

[7] D. N. Spergel *et al.*, Astrophys. J. Suppl. Ser. **170**, 377 (2007).

[8] E. Komatsu *et al.*, Astrophys. J. Suppl. Ser. **180**, 330 (2009).

[9] H. K. Eriksen, A. J. Banday, K. M. Górski, and P. B. Lilje, Astrophys. J. **622**, 58 (2005); P. D. Naselsky, L.-Y. Chiang, P. Olesen, and O. V. Verkhodanov, Astrophys. J. **615**, 45 (2004); P. Coles, P. Dineen, J. Earl, and D. Wright, Mon. Not. R. Astron. Soc. **350**, 989 (2004); P. D. Naselsky, O. V. Verkhodanov, L.-Y. Chiang, and I. Novikov, Int. J. Mod. Phys. D **14**, 1273 (2005); P. Naselsky, L.-Y. Chiang, P. Olesen, and I. Novikov, Phys. Rev. D **72**, 063512 (2005); K. Land and J. Magueijo, Mon. Not. R. Astron. Soc. **362**, L16 (2005); P. Cabella, M. Liguori, F. K. Hansen, D.

Marinucci, S. Matarrese, L. Moscardini, and N. Vittorio, Mon. Not. R. Astron. Soc. **358**, 684 (2005); M. Liguori, F. K. Hansen, E. Komatsu, S. Matarrese, and A. Riotto, Phys. Rev. D **73**, 043505 (2006); P. Cabella, F. K. Hansen, M. Liguori, D. Marinucci, S. Matarrese, L. Moscardini, and N. Vittorio, Mon. Not. R. Astron. Soc. **369**, 819 (2006); C. Hikage, T. Matsubara, P. Coles, M. Liguori, F. K. Hansen, and S. Matarrese, Mon. Not. R. Astron. Soc. **389**, 1439 (2008); B. Lew, J. Cosmol. Astropart. Phys. 08 (2008) 017.

[10] L.-Y. Chiang, P. D. Naselsky, O. V. Verkhodanov, and M. J. Way, Astrophys. J. **590**, L65 (2003).

[11] P. D. Naselsky, L.-Y. Chiang, I. D. Novikov, and O. V. Verkhodanov, Int. J. Mod. Phys. D **14**, 1273 (2005).

[12] H. K. Eriksen, F. K. Hansen, A. J. Banday, K. M. Górski, and P. B. Lilje, Astrophys. J. **605**, 14 (2004).

[13] P. Vielva, E. Martínez-González, R. B. Barreiro, J. L. Sanz, and L. Cayón, Astrophys. J. **609**, 22 (2004); M. Cruz, E. Martínez-González, P. Vielva, and L. Cayón, Mon. Not. R. Astron. Soc. **356**, 29 (2005); M. Cruz, L. Cayón, E. Martínez-González, P. Vielva, and J. Jin, Astrophys. J. **655**, 11 (2007); L. Cayón, J. Jin, and A. Treaster, Mon. Not. R. Astron. Soc. **362**, 826 (2005); Lung-Y Chiang and P. D. Naselsky, Int. J. Mod. Phys. D **15**, 1283 (2006); J. D. McEwen, M. P. Hobson, A. N. Lasenby, and D. J. Mortlock, Mon. Not. R. Astron. Soc. **359**, 1583 (2005); **371**, L50 (2006); **388**, 659 (2008); A. Bernui, C. Tsallis, and T. Villela, Europhys. Lett. **78**, 19001 (2007); Phys. Lett. A **356**, 426 (2006); L.-Y. Chiang, P. D. Naselsky, and P. Coles, Astrophys. J. **664**, 8 (2007); C.-G. Park, Mon. Not. R. Astron. Soc. **349**, 313 (2004); D. L. Larson and B. D. Wandelt, Astrophys. J. **613**, L85 (2004); H. K. Eriksen, D. I. Novikov, P. B. Lilje, A. J. Banday, and K. M. Górski, Astrophys. J. **612**, 64 (2004); C. J. Copi, D. Huterer, and G. D. Starkman, Phys. Rev. D **70**, 043515 (2004); C. J. Copi, D. Huterer, D. J. Schwarz, and G. D. Starkman, Mon. Not. R. Astron. Soc. **367**, 79 (2006); T. R. Jaffe, A. J. Banday, H. K. Eriksen, K. M. Górski, and F. K. Hansen, Astrophys. J. **629**, L1 (2005); M. Cruz, M. Tucci, E. Martínez-González, and P. Vielva, Mon. Not. R. Astron. Soc. **369**, 57 (2006); M. Cruz, N. Turok, P. Vielva, E. Martínez-González, and M. Hobson, Science **318**, 1612 (2007); K. Land and J. Magueijo, Mon. Not. R. Astron. Soc. **357**, 994 (2005); F. K. Hansen, P. Cabella, D. Marinucci, and N. Vittorio, Astrophys. J. **607**, L67 (2004); P. Mukherjee and Y. Wang, Astrophys. J. **613**, 51 (2004); D. Pietrobon, P. Cabella, A. Balbi, G. de Gasperis, and N. Vittorio, arXiv:0812.2478; P. Vielva and J. L. Sanz, arXiv:0812.1756; P. K. Samal, R. Saha, P. Jain, and J. P. Ralston, arXiv:0811.1639.

[14] E. Martínez-González, arXiv:0805.4157; Y. Wiaux, P. Vielva, E. Martínez-González, and P. Vandergheynst, Phys. Rev. Lett. **96**, 151303 (2006); C. J. Copi, D. Huterer, D. J. Schwarz, and G. D. Starkman, Phys. Rev. D **75**, 023507 (2007); L. R. Abramo, A. Bernui, I. S. Ferreira, T. Villela, and C. A. Wuensche, Phys. Rev. D **74**, 063506 (2006); D. Huterer, New Astron. Rev. **50**, 868 (2006); P. Vielva, Y. Wiaux, E. Martínez-González, and P. Vandergheynst, New Astron. Rev. **50**, 880 (2006); Mon. Not. R. Astron. Soc. **381**, 932 (2007); H. K. Eriksen, A. J. Banday, K. M. Górski, F. K. Hansen, and P. B. Lilje, Astrophys. J. **660**, L81 (2007); K. Land and J. Magueijo, Mon. Not. R. Astron. Soc. **378**, 153 (2007); A. Bernui, B. Mota, M. J. Rebouças, and R. Tavakol, Astron. Astrophys. **464**, 479 (2007); Int. J. Mod. Phys. D **16**, 411 (2007); T. Kahniashvili, G. Lavrelashvili, and B. Ratra, Phys. Rev. D **78**, 063012 (2008); B. Lew, J. Cosmol. Astropart. Phys. 09 (2008) 023; A. Bernui, Phys. Rev. D **78**, 063531 (2008); F. K. Hansen, A. J. Banday, and K. M. Górski, Mon. Not. R. Astron. Soc. **354**, 641 (2004); F. K. Hansen, P. Cabella, D. Marinucci, and N. Vittorio, Astrophys. J. **607**, L67 (2004); P. Bielewicz, K. M. Górski, and A. J. Banday, Mon. Not. R. Astron. Soc. **355**, 1283 (2004); K. Land and J. Magueijo, Phys. Rev. Lett. **95**, 071301 (2005); A. Bernui, T. Villela, C. A. Wuensche, R. Leonardi, and I. Ferreira, Astron. Astrophys. **454**, 409 (2006); M. Tegmark, A. de Oliveira-Costa, and A. J. S. Hamilton, Phys. Rev. D **68**, 123523 (2003); A. de Oliveira-Costa, M. Tegmark, M. Zaldarriaga, and A. Hamilton, Phys. Rev. D **69**, 063516 (2004); J. R. Weeks, arXiv:astro-ph/0412231; P. Bielewicz, H. K. Eriksen, A. J. Banday, K. M. Górski, and P. B. Lilje, Astrophys. J. **635**, 750 (2005).

[15] B. Gold *et al.*, Astrophys. J. Suppl. Ser. **180**, 265 (2009).

[16] G. Hinshaw *et al.*, Astrophys. J. Suppl. Ser. **170**, 288 (2007); **180**, 225 (2009).

[17] K. M. Górski, E. Hivon, A. J. Banday, B. D. Wandelt, F. K. Hansen, M. Reinecke, and M. Bartelman, Astrophys. J. **622**, 759 (2005).

[18] D. N. Spergel *et al.*, Astrophys. J. Suppl. Ser. **170**, 377 (2007).

[19] J. Kim, P. Naselsky, and P. R. Christensen, Phys. Rev. D **77**, 103002 (2008).

[20] C.-G. Park, C. Park, and J. R. Gott, III, Astrophys. J. **660**, 959 (2007).

[21] A. de Oliveira-Costa and M. Tegmark, Phys. Rev. D **74**, 023005 (2006). CMB multipole measurements in the presence of foregrounds.